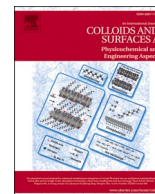




Contents lists available at ScienceDirect

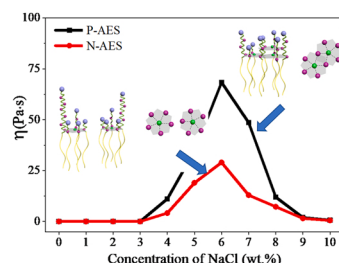
Colloids and Surfaces A: Physicochemical and Engineering Aspects

journal homepage: www.elsevier.com/locate/colsurfa

Enhanced salt thickening effect of the aqueous solution of peaked-distribution alcohol ether sulfates (AES)

Xiao Xiao^a, Jinwan Qi^a, Jingjie Zhou^b, Yongqiang Sun^b, Jianbin Huang^{a,*}, Yun Yan^{a,*}^a Beijing National Laboratory for Molecular Sciences (BNLMS), State Key Laboratory for Structural Chemistry of Unstable and Stable Species, College of Chemistry and Molecular Engineering, Peking University, Beijing 100871, PR China^b China Research Institute of Daily Chemistry Co., Ltd, Taiyuan 03001, PR China

GRAPHICAL ABSTRACT



The Na⁺ binds with EO groups of in peaked-distribution AES (P-AES) more efficiently than in normal-distribution AES (N-AES), resulting enhanced thickening effect.

ARTICLE INFO

Keywords:

Salt-thickening
Alcohol ether sulfates
Surfactant
Wormlike micelle, Viscosity

ABSTRACT

Alcohol Ether Sulfates (AES) are emerging as a potent category of surfactant in consumer product industry owing to their much better hard water resistance, foaming/wetting ability, and less irritating than alkyl sulfate. These excellent performances are attributed to the presence of oxyethylene (EO) chain between the hydrophilic and the hydrophobic portions which endows AES the combined advantages of both nonionic and anionic surfactants. Most strikingly, addition of NaCl would considerably enhance the viscosity of the aqueous solution of AES, which is very important for a better retention of the surfactant to the interacting substrate. Recent study shows that the number distribution of EO groups considerably affects this salt-thickening performance, yet its mechanism is not clear. We report in this work that the narrower number distribution of the EO groups in the AES chains would generate an order alignment of the stretched EO chains, which can then bind with Na⁺ efficiently to form supramolecular crown ethers. In contrast, as the EO numbers are polydispersed, it is hard for them to align orderly, resulting in poor supramolecular crown ether formation ability with Na⁺. As a result, the wormlike micelles formed in the AES with narrower EO number distribution has much pronounced salt-thickening effect. This finding may help people in relating fields to create products with desired performance.

* Corresponding authors.

E-mail addresses: jbhuang@pku.edu.cn (J. Huang), yunyan@pku.edu.cn (Y. Yan).

<https://doi.org/10.1016/j.colsurfa.2021.128146>

Received 9 November 2021; Received in revised form 10 December 2021; Accepted 16 December 2021

Available online 20 December 2021

0927-7757/© 2021 Published by Elsevier B.V.

1. Introduction

Surfactants are a kind of amphiphiles with strong surface activity. Because of their functions in wetting, emulsification, foaming and solubilization, they are widely used in various fields, such as oilfield industry [1], food industry [2], nanotechnology [3], medicine and biotechnology [4,5], as well as in chemical industry for daily use [6,7]. Particularly, the surfactants for daily use need to display good washing effect, small skin irritation and environmental friendliness. Alcohol ether sulfates (AES) is a kind of such surfactants with a dodecyl chain tethered to a sulfate head by several ethylene oxide groups. The coexistence of both sulfate and ethylene oxide groups renders AES the combined advantages of anionic and nonionic surfactants [8,9], which has attracted increasing attention in consumer product industry [10].

For the production of consumer products, sufficiently high viscosity is required to have better retention time on the applied surface. The viscosity of most products made with ionic surfactants can be promoted by shielding the electrostatic repulsions with inorganic salts. The viscosity of the aqueous solution of AES displays salt thickening effect as well [11]. However, it still remains challenging to further promote the viscosity of the AES solution with the same amount of inorganic salt. Because the number of the ethylene oxide (EO) in the chain of AES is not well-defined¹², the entire chain lengths of AES molecules are different from each other in the same batch. As a result, the AES molecules in the wormlike micelles cannot arrange very orderly, leading to poor networks [12]. We assume that if the distribution of the EO groups in the AES system is narrowed, the salt-thickening effect of the AES surfactant would be enhanced noticeably, promoting its performance in consumer products.

Herein we report that this scenario indeed occurs. We show that the viscosity of the AES with a narrower EO distribution [13], which is termed with P-AES, is over 2 times of that of ordinary AES upon addition of the same amount of NaCl. This significantly enhanced viscosity allows generating better retention time, thus promotes the cleaning ability. Owing to the peaked-distribution of the EO groups, the entire-length of the molecules in the wormlike micelles are close to each other, so that they arrange more orderly than those formed with ordinary AES. As a result, the Na⁺ ions of NaCl are capable to cross-link the EO groups from different AES molecules via the formation of a pseudo “crown ether” [14], which we term as supramolecular crown ether, thus leading to a denser network that increases the viscosity.

2. Experimental section

2.1. Materials

Two series of commercial AES were obtained from China Research Institute of Daily Chemical Industry. The other chemicals were obtained from Beijing Chemical Reagents Co. and were all of A.R. grade. Distilled water was purified through a Milli-Q Advantage A10 ultrapure water system.

2.2. Sample preparation

The samples were prepared by vortex mixing AES stock solution and NaCl solution, kept in 25 °C incubator at least 24 h before testing. The concentration for all solutions was expressed in weight percent (wt%). The final concentration of AES used in this study was 10%, and NaCl was from 0 wt% to 10 wt%.

2.3. Rheological measurements

The rheological measurements were performed by a Thermo Haake RS300 with a double-gap cylinder sensor (DG 41) or a cone-plate sensor (PP35 Ti). It could be chosen according to the fluidity of the sample. The double-gap cylinder sensor was used in low viscosity systems (< 1 Pa s)

and cone-plate sensor was for high viscous system. All measurements were performed at 25 °C, controlled by a Thermo Haake C25P controller. The viscous properties were obtained by steady-state measurements, and the viscoelastic measurements were performed by oscillatory measurements from 0.1 to 10 Hz, ensuring the deformation was controlled in linear region.

2.4. Transmission electron microscopy (TEM)

TEM images were recorded on JEM-2100F Field-emission High Resolution Transmission Electron Microscope (Japan, 200kv). The samples were prepared by dropping solutions onto copper grids coated with the Formvar film. Excess water was removed by a filter paper, and the samples were dried in an ambient environment at room temperature for TEM observation.

2.5. X-ray diffraction (XRD)

Reflection XRD studies were performed using a model XKS-2000 X-ray diffractometer (Scintaginc). The X-ray wavelength was obtained from a Cu K α beam ($\lambda = 1.5406 \text{ \AA}$) generated with a Cu anode.

2.6. Surface tension measurements

Dynamic Contact Angle Analyzer DCA-315(CAHN) performed the surface tension measurements at 25 °C. All solutions were prepared before texting at least 24 h.

3. Results and discussions

3.1. Basic information about the two AES samples

Table 1 shows the composition of the peaked-distribution AES (P-AES) and the ordinary distribution AES (O-AES). The fraction of AES with inserted EO groups ranging from 1 to 3 is as high as 58 wt% in the P-AES system, whereas that in the O-AES system is only 42 wt%. Furthermore, the number of EO groups in P-AES system is more uniform, representing by the closed content of AES with 1, 2, and 3 EO group being 20 wt%, 22 wt%, and 16 wt%. In contrast, the corresponding EO number distribution in the ordinary AES system is 20 wt%, 13 wt%, and wt.9%, respectively.

The aqueous solution of P-AES and O-AES has nearly the same surface properties and viscosity (Fig. S1). Addition of NaCl decreases the CMC and surface tension of the two AES solutions to the same extent (Fig. S1), and the maximum zero-shear viscosity occurs at similar NaCl concentrations (Fig. 1). However, the maximum zero-shear viscosity for the P-AES is over two times of that of the O-AES at the same concentration of NaCl, indicating the P-AES displays much better salt-thickening effect.

Table 1

The number of EO groups in the alcohol ether (AEO-n, n denotes the number of EO group). AEO will transform into AES after sulfonation. As n = 0, the sulfonation leads to formation of sodium dodecyl sulfonate(SDS).

	P-AES (wt%)	O-AES (wt%)
SDS	32.8873	45.0386
AEO-1	20.3221	20.3738
AEO-2	22.3912	13.7647
AEO-3	16.132	9.005
AEO-4	6.4922	5.5305
AEO-5	1.4678	3.0829
AEO-6	0.2282	1.5652
AEO-7	–	0.5949

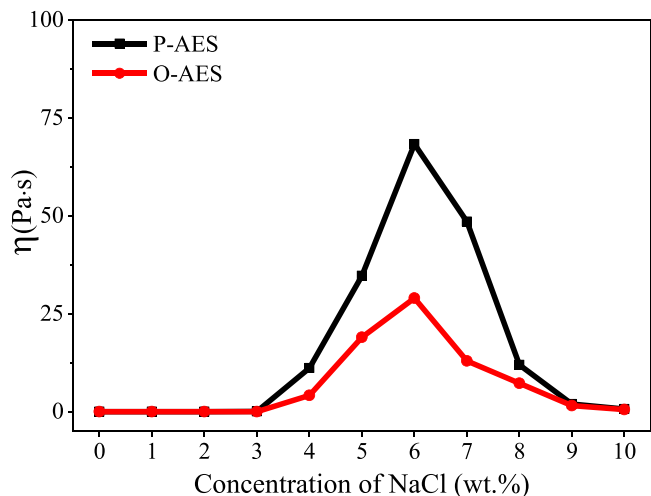


Fig. 1. The zero-shear viscosity of 10 wt% P-AES (black) and O-AES (red) after adding NaCl.

3.2. Rheological properties of the two salt-thickened AES solutions

To reveal more structural insight, dynamic rheological measurements were performed for the two series of AES solutions with different NaCl concentrations, and the results are given in Figs. 2 and S2. All the

thickened systems are featured by characters of visco-elastic fluids. At low frequencies(f), the viscous modulus G'' is dominant over the elastic one, whereas the elastic modulus G' becomes dominant at higher frequencies. At frequencies below the crossover G' and G'' , the $G'-f$, $G''-f$ curves in the logarithmic coordinates are nearly linear correlation, and the complex viscosity $|\eta^*|$ is a constant, featuring the formation of wormlike micelles in all these salt-thickened systems [15]. In this region, G' and G'' can be well fitted to the Maxwell model [16]:

$$G'(\omega) = \frac{G_0(\omega \bullet \tau_R)^2}{1 + (\omega \bullet \tau_R)^2} \quad (1)$$

$$G''(\omega) = \frac{G_0\omega \bullet \tau_R}{1 + (\omega \bullet \tau_R)^2} \quad (2)$$

$$G''^2 + \left(G' - \frac{1}{2}G_0\right)^2 = \frac{1}{4}G_0^2 \quad (3)$$

where G_0 is the plateau modulus and τ_R is the relaxation time. Eq. (3) can be derived from Eqs. (1) and (2). The value of τ_R is calculated as the reciprocal of the frequency f , $1/2\pi f$, which is obtained from the crossover of G' and G'' . It is noticed that the crossover in the P-AES system always occurs at a much lower frequency f for the same NaCl concentration, indicating the relaxation time τ_R is much longer. Table 2 records the experimental results obtained from Fig. 2, which reveals that the longer relaxation time is always accompanied by a larger viscosity. According to the theoretical description of the rheological behaviors for

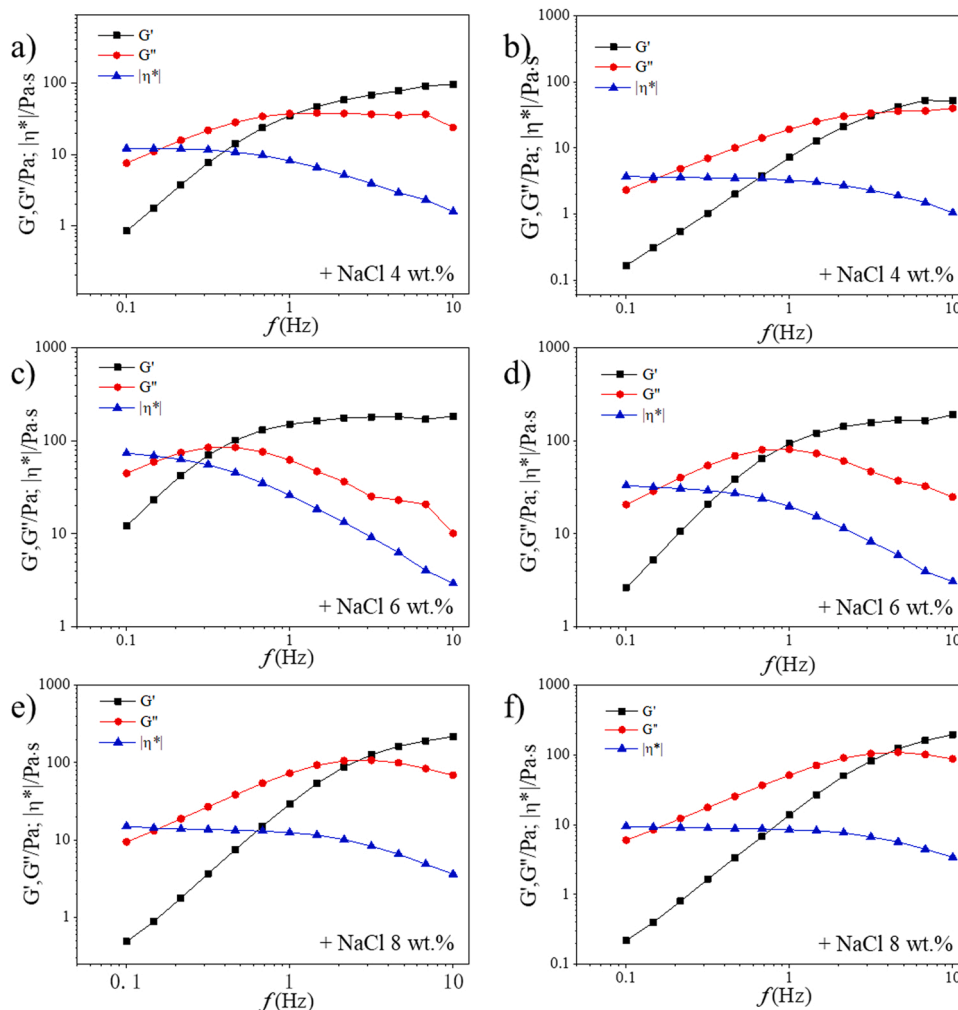


Fig. 2. Small amplitude oscillatory rheology of 10 wt% P-AES(a/c/e) and O-AES (b/d/f) with adding 4 wt%–8 wt% NaCl.

Table 2

The zero-shear viscosity (η_0) and relaxation time (τ_R) of P-AES and O-AES systems with NaCl.

Concentration of NaCl	P-AES		O-AES	
	η (Pa s)	τ_R (s)	η (Pa s)	τ_R (s)
4 wt%	11.14	0.145	4.2	0.045
6 wt%	68.32	0.4	29	0.185
8 wt%	12.02	0.06	7.3	0.039

wormlike micelles firstly reported by Cates, the longer τ_R is always corresponding to a high viscosity, which is resulted from the denser networks formed by wormlike micelles [11]. This means that denser networks are formed in the P-AES system.

Further analysis of the rheograms was performed by taking G' as the abscissa and G'' as the ordinate to obtain a Cole-Cole plot. Fig. 3 shows the Cole-Cole plot for both systems. Semicircles with $1/2G_0$ as the center were obtained at different NaCl concentrations. G_0 is a parameter describing the density of the network structure of the system, which is inversely proportional to the mesh size of the network. In Fig. 3, the G_0 of peaked-distribution systems increase with increasing the concentration of NaCl for 4–8 wt%, indicating that the network structure is becoming denser. This means that binding of Na^+ to P-AES continues as the concentration of NaCl increases from 4 wt to 8 wt%. At high frequencies, the plots deviate the theoretical Maxwell model. This phenomenon has been reported in many viscoelastic surfactant solutions, which is probably resulted from the “breathe modes” [15]. However, in O-AES system, the mesh size does not increase noticeably as the concentration of NaCl reaches a certain value (5 wt%), indicating binding of Na^+ to O-AES reaches equilibrium at about 5 wt% NaCl. Clearly, at the same NaCl concentration, the P-AES generally has a smaller mesh network size. It is noticed that the maximum viscosity occurs at 6 wt% NaCl for both systems, whereas the maximum G_0 occurs at 8 wt% NaCl. Similar phenomenon was also reported by other groups [11], which is attributed to the formation of structures with higher elasticity induced by higher NaCl concentration.

3.3. TEM study of the wormlike micelles formed in the two salt-thickened AES solutions

The structural difference between the micelles formed in the two surfactant systems was further characterized by TEM. Fig. 4 shows the TEM images for the two systems with different NaCl concentrations. The upper and lower rows in Fig. 4 are the TEM image for the wormlike micelles in the P- and O-AES systems, respectively, with increasing NaCl concentration. It is clear that the network density of the wormlike micelles in the P-AES system (Fig. 4a/b) is significantly higher than that in the O-AES system (Fig. 4c/d) at both 4 wt% and 6 wt% NaCl, verifying that the enhanced salt-thickening effect in the P-AES system is originated from the strengthened networks of wormlike micelles.

3.4. Molecular origin of the enhanced salt-thickening ability of the P-AES

The molecular origin of the significantly enhanced salt-thickening effect in the P-AES system than the O-AES is attributed to the different binding ability of EO chains with Na^+ . Alkaline metal ions are able to form pseudo-crown ether structures with poly EO [13,17,18]. Usually, it takes 5 EO to bind with 1 alkaline metal ions [17,18]. However, in case of the absence of poly EO, one alkaline metal ion is able to bind with 5 EO from 5 parallelly arranged molecules [19], as illustrated in Scheme 1a. Because the dominant number of EO groups per AES chain is in the range of 1–4, which sums to nearly 65 wt% over the entire composition. Specially, the AES chains with 1, 2, and 3 EO groups are concentrated at the close portions of 20 wt%, 22 wt%, and 16 wt%. This renders a relatively smooth hydrophilic surface for the resultant wormlike micelles (Scheme 1b). As a result, it is easier to find 5 EO groups from 5 neighboring AES molecules to bind with 1 Na^+ to form a “supramolecular crown ether”, as illustrated in the enlarged window in Scheme 1b. In contrast, the number of EO groups per AES chain in the O-AES chains are rather polydisperse (Table 1). As a comparison, the AES chains with 1, 2, and 3 EO groups in the P-AES system are 20 wt%, 14 wt%, 9 wt%, respectively. However, the number distribution of EO groups in the O-AES system is rather wide. Table 1 shows that there are even considerable portion of AES with 4, 5, 6, and 7 EOs. The quite wide EO number distribution in the O-AES systems makes it impossible to have wormlike micelles with smooth hydrophilic surfaces (Scheme 1c). As a result, it is hard to find 5 neighboring EO groups at the same latitude to form similar supramolecular crown ethers, as illustrated in the enlarged windows in Scheme 1c. This means that binding of Na^+ in the O-AES system is not as efficient as that in the P-AES system, which explains why the cole-cole plots in Fig. 3b for the O-AES systems almost overlap with each other as the concentration of NaCl exceeds 5 wt%. Furthermore, the significantly large fraction of SDS in the O-AES system (Table 1) than in the P-AES system is also disadvantageous for the binding of Na^+ . The data in Table 1 clearly shows that the weight fraction of SDS in the P-AES and O-AES system is $\sim 32\%$ and 45% , respectively; in line with this, the overall weight fraction of AES in the P-AES and O-AES system is $\sim 67\%$ and 54% , respectively. Since SDS has only one sulfate group to bind with Na^+ electrostatically, it is obvious that the significantly larger fraction of AES in the P-AES system has much stronger Na^+ binding ability than O-AES owing to the extra formation of supramolecular crown ethers.

Since the binding of Na^+ would introduce positive charges to the electroneutral EO portion, it will generate repulsion. As a result, the bilayer thickness will increase. The XRD patterns in Fig. 5a shows that the bilayer thickness in the P-AES system increases from 4.01 to 4.12 nm upon addition of 4 wt% NaCl, but the bilayer thickness noticeably decreases to 4.09 nm as further increasing the NaCl concentration to 6 wt% and 8 wt% (Fig. 5a), which is due to shielding effect. In contrast, addition of 4 wt% NaCl to the O-AES system will significantly reduce the bilayer thickness from 4.35 to 4.09 nm (Fig. 5b), indicating NaCl prefers to shield the negative charges on the sulfate groups. This means that the

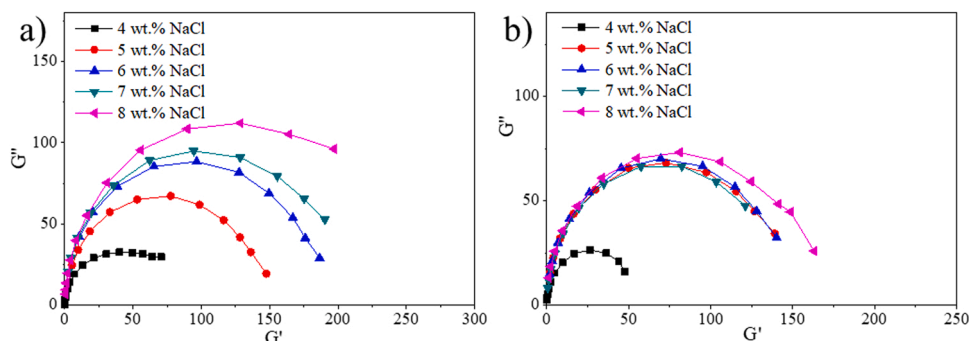


Fig. 3. Cole-Cole plots of P-AES (a) and O-AES (b).

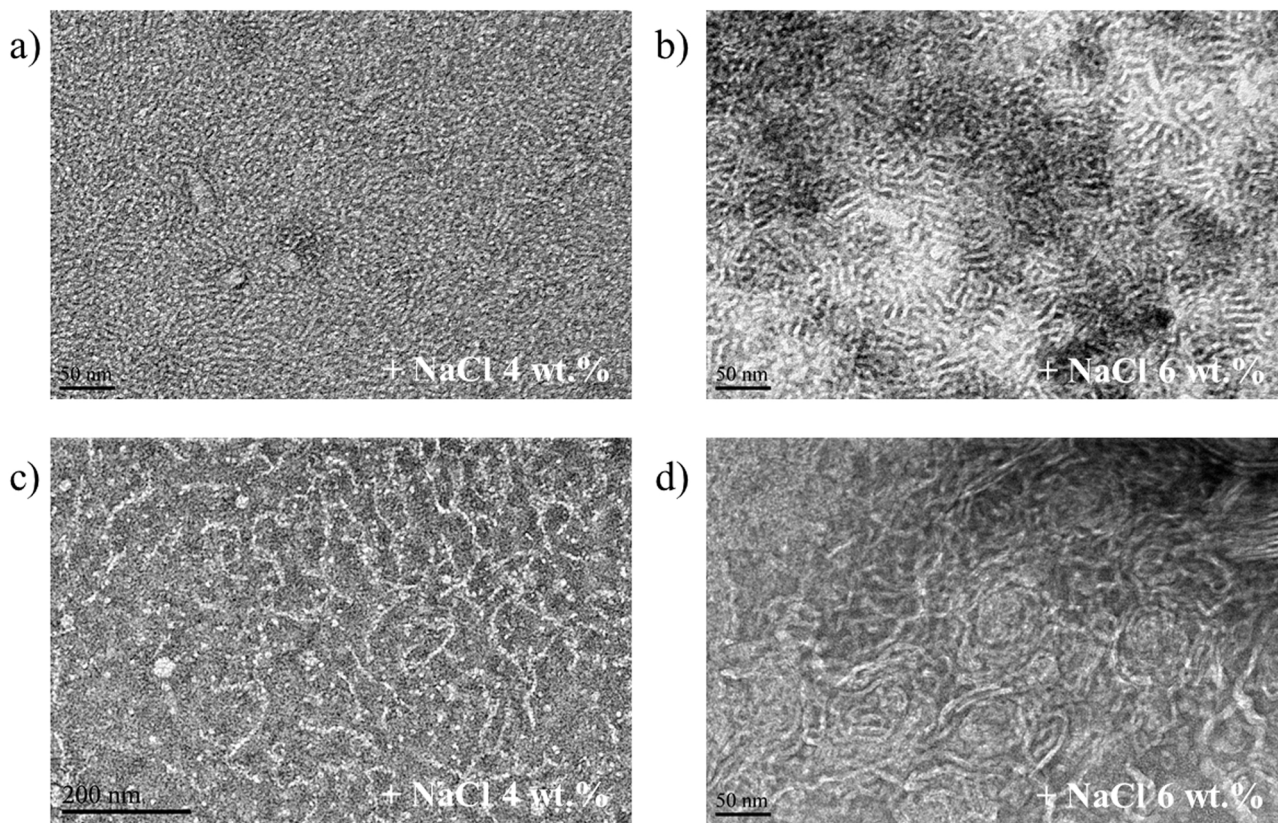
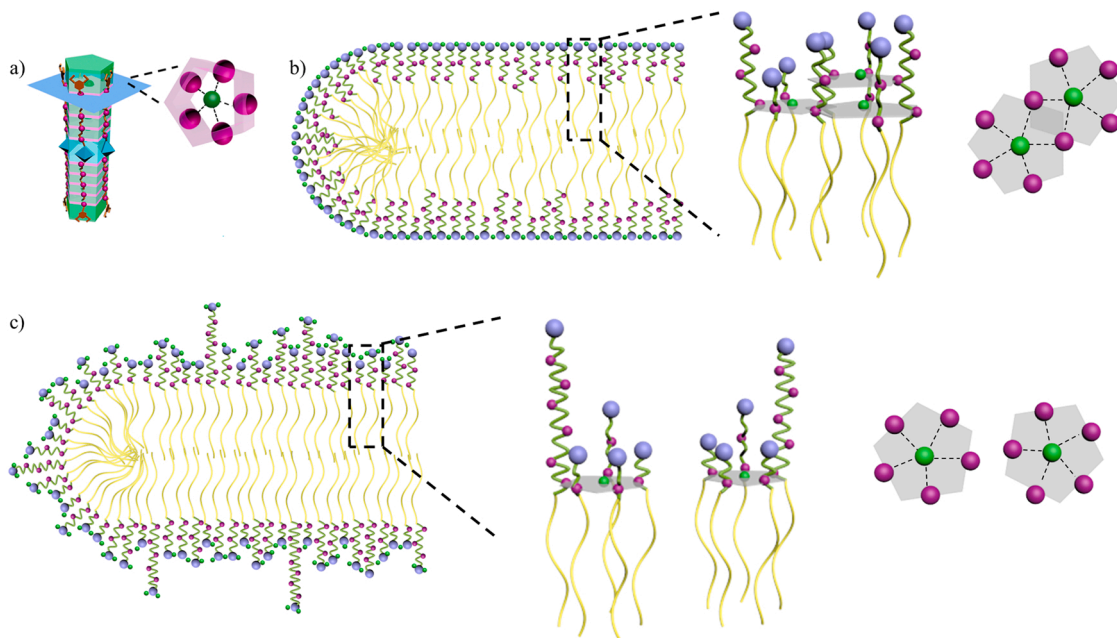


Fig. 4. TEM of P-AES(a/b) and O-AES (c/d) with adding 4 wt% and 6 wt% NaCl.



Scheme 1. (a) Illustration of the binding mode for one Li^+ (green sphere) with five O (pink spheres) from five TPE-(EO)₄-L₂ molecules [19]. (b) Smoother surfaces caused by close EO chain lengths for the wormlike micelles in the P-AES system. The enlarged window shows the binding on Na^+ (green sphere) with 5 EO (green chain and pink spheres) at the same latitude from neighboring 5 AES to form supramolecular crown ethers, and the share of EO chains by two supramolecular crown ether clusters. (c) Coarser surface caused by the different EO chain lengths for the wormlike micelles in the O-AES system. The enlarged window shows the binding of Na^+ with separate supramolecular crown ether clusters.

disorderly arranged EO groups on the coarse surface of the wormlike micelles has poor ability of binding Na^+ , so that the added NaCl would prefer to shield the electrostatic charges on the sulfate groups. After that,

binding of Na^+ to from supramolecular crown ether would occur, which is reflected in the nearly constant bilayer thickness at the 4 wt% and 6 wt% NaCl, but the noticeably increased bilayer thickness at 8 wt%

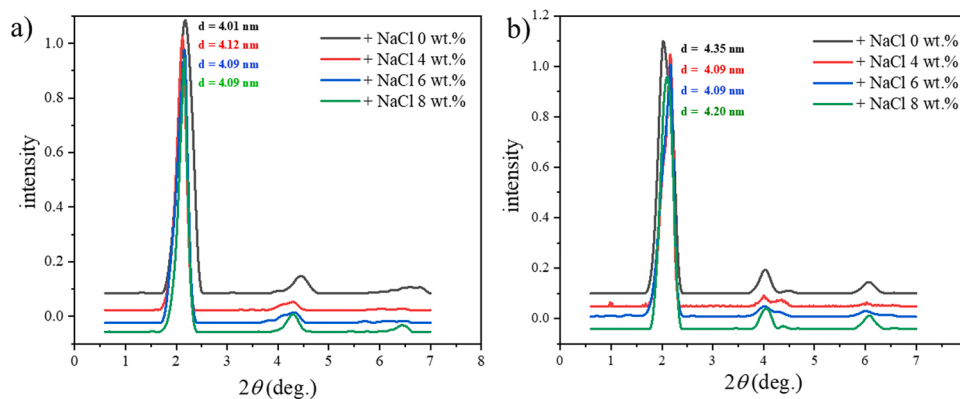


Fig. 5. XRD patterns of P-AES (a) and O-AES (b) with different concentrations of NaCl.

NaCl (Fig. 5b).

It should be pointed out that in case of no additional NaCl, the smaller bilayer thickness in the P-AES system (4.01 nm) than the O-AES system (4.35 nm) reflects the lack of long EO chains in the P-AES system. This is understandable since the long EO chains will increase the stretching length of the AES molecule. Furthermore, the narrower EO number distribution in the P-AES system also enables two binding clusters to share EO chains, as illustrated in Scheme 1b, which generates stiffer and denser networks. However, such a scenario can hardly occur in the O-AES system. For this reason, the salt-thickening effect is weaker in the O-AES system than the P-AES system.

4. Conclusion

In summary, we conclude that the enhanced salt-thickening effect in the P-AES system is attributed to the narrowed number distribution of the EO groups in the AES chain. The formation of supramolecular crown ether structure would be much easier upon addition of extra NaCl in the P-AES system, so that stiffening of the wormlike AES micelles becomes possible, leading to enhanced salt thickening effect.

CRediT authorship contribution statement

Xiao Xiao: Conducted most of the experiments, Writing – original draft. **Jinwan Qi:** Repeated the experiments and provided final XRD data. **Jingjie Zhou:** Synthesized the AES. **Yongqiang Sun:** Supervision, designed the AES synthesis. **Jianbin Huang:** Discussed the results and analyzed the data. **Yun Yan:** Designed the study, analyzed the data and revised the paper.

Declaration of Competing Interest

The authors declare that they have no known competing financial interests or personal relationships that could have appeared to influence the work reported in this paper.

Acknowledgments

This work is financially supported by the National Key Research and Development Program of China (2017YFB0308800).

Appendix A. Supplementary material

Supplementary data associated with this article can be found in the

online version at doi:10.1016/j.colsurfa.2021.128146.

References

- [1] A. Bera, S. Kissmathulla, K. Ojha, T. Kumar, A. Mandal, Mechanistic study of wettability alteration of quartz surface induced by nonionic surfactants and interaction between crude oil and quartz in the presence of sodium chloride salt, *Energy Fuels* 26 (2012) 3634–3643.
- [2] I. Kralova, J. Sjöblom, Surfactants used in food industry: a review, *J. Dispers. Sci. Technol.* 30 (2009) 1363–1383.
- [3] C. Faure, A. Derré, W. Neri, Spontaneous formation of silver nanoparticles in multilamellar vesicles, *J. Phys. Chem. B* 107 (2003) 4738–4746.
- [4] M. El-Badry, G. Fetih, M. Fathy, Improvement of solubility and dissolution rate of indomethacin by solid dispersions in Gelucire 50/13 and PEG4000, *Saudi Pharm. J.* 17 (2009) 217–225.
- [5] K.M.G. Taylor, D.Q.M. Craig, Liposomes for drug delivery: developments and possibilities, *Int. J. Pharm. Pract.* 2 (1993) 128–135.
- [6] W.W. Schmidt, D.R. Durante, R. Gingell, J.W. Harbell, Alcohol ethoxycarboxylates – mild, high-foaming surfactants for personal-care products, *JAOCS J. Am. Oil Chem. Soc.* 74 (1997) 25–31.
- [7] J.J. Scheibel, The evolution of anionic surfactant technology to meet the requirements of the laundry detergent industry, *J. Surfactants Deterg.* 7 (2004) 319–328.
- [8] S.D. Dyer, D.T. Stanton, J.R. Lauth, D.S. Cherry, Structure-activity relationships for acute and chronic toxicity of alcohol ether sulfates, *Environ. Toxicol. Chem.* 19 (2000) 608–616.
- [9] E. Matthijs, M.S. Holt, A. Kiewiet, G.B.J. Rijs, Environmental monitoring for linear alkylbenzene sulfonate, alcohol ethoxylate, alcohol ethoxy sulfate, alcohol sulfate, and soap, *Environ. Toxicol. Chem. Int. J.* 18 (1999) 2634–2644.
- [10] H. Watanabe, W.L. Groves, Alcohol ether sulfates in shampoos, *J. Am. Oil Chem. Soc.* 45 (1968) 738–741.
- [11] J.H. Mu, G.Z. Li, X.L. Jia, H.X. Wang, G.Y. Zhang, Rheological properties and microstructures of anionic micellar solutions in the presence of different inorganic salts, *J. Phys. Chem. B* 106 (2002) 11685–11693.
- [12] D.L. Smith, Comparison of salt thickening of conventional and peaked alcohol ether sulfates, *J. Am. Oil Chem. Soc.* 68 (1991) 629–633.
- [13] M.F. Cox, The effect of “peaking” the ethylene oxide distribution on the performance of alcohol ethoxylates and ether sulfates, *J. Am. Oil Chem. Soc.* 67 (1990) 599–604.
- [14] Y. Lu, S.T. Kong, H.J. Deiseroth, W. Mormann, Structural requirements for the intercalation of polyether polyols into sodium-montmorillonite: the role of oxyethylene sequences, *Macromol. Mater. Eng.* 293 (2008) 900–906.
- [15] H. Fan, Y. Yan, Z. Li, Y. Xu, L. Jiang, L. Xu, B. Zhang, J. Huang, General rules for the scaling behavior of linear wormlike micelles formed in catanionic surfactant systems, *J. Colloid Interface Sci.* 348 (2010) 491–497.
- [16] M.E. Cates, Nonlinear viscoelasticity of wormlike micelles (and other reversibly breakable polymers), *J. Phys. Chem.* 94 (1990) 371–375.
- [17] P. Johansson, J. Tegenfeldt, J. Lindgren, Modelling amorphous lithium salt-PEO polymer electrolytes: ab initio calculations of lithium ion-tetra-, penta- and hexaglyme complexes, *Polymer* 40 (1999) 4399–4406.
- [18] D. Diddens, A. Heuer, O. Borodin, Understanding the lithium transport within a rouse-based model for a PEO/LiTFSI polymer electrolyte, *Macromolecules* 43 (2010) 2028–2036.
- [19] R. Xue, Y. Han, Y. Xiao, J. Huang, B.Z. Tang, Y. Yan, Lithium ion nanocarriers self-assembled from amphiphiles with aggregation-induced emission activity, *ACS Appl. Nano Mater.* 1 (2018) 122–131.